Physics Letters B 767 (2017) 226–231

Contents lists available at ScienceDirect

Physics Letters B

www.elsevier.com/locate/physletb

Empirical moments of inertia of axially asymmetric nuclei

J.M. Allmond [a,*], J.L. Wood [b]

[a] Physics Division, Oak Ridge National Laboratory, Oak Ridge, TN 37831, USA
[b] School of Physics, Georgia Institute of Technology, Atlanta, GA 30332, USA

ARTICLE INFO

Article history:
Received 18 August 2016
Received in revised form 4 November 2016
Accepted 15 January 2017
Available online 6 February 2017
Editor: D.F. Geesaman

ABSTRACT

Empirical moments of inertia, $\mathcal{J}_1$, $\mathcal{J}_2$, $\mathcal{J}_3$, of atomic nuclei with $E(4_1^+)/E(2_1^+) > 2.7$ are extracted from experimental $2^+_{g,\gamma}$ energies and electric quadrupole matrix elements, determined from multi-step Coulomb excitation data, and the results are compared to expectations based on rigid and irrotational inertial flow. Only by having the signs of the $E2$ matrix elements, i.e., $\langle 2^+_g||\hat{M}(E2)||2^+_g\rangle$ and $\langle 0^+_g||\hat{M}(E2)||2^+_g\rangle\langle 2^+_g||\hat{M}(E2)||2^+_\gamma\rangle\langle 2^+_\gamma||\hat{M}(E2)||0^+_g\rangle$, can a unique solution to all three components of the inertia tensor of an asymmetric top be obtained. While the absolute moments of inertia fall between the rigid and irrotational values as expected, the relative moments of inertia appear to be qualitatively consistent with the $\beta^2\sin^2(\gamma)$ dependence of the Bohr Hamiltonian which originates from a SO(5) invariance. A better understanding of inertial flow is central to improving collective models, particularly hydrodynamic-based collective models. The results suggest that a better description of collective dynamics and inertial flow for atomic nuclei is needed. The inclusion of vorticity degrees of freedom may provide a path forward. This is the first report of empirical moments of inertia for all three axes and the results should challenge both collective and microscopic descriptions of inertial flow.

Atomic nuclei are finite many-body quantum systems composed of strongly interacting fermions that share remarkable similarities with other systems such as molecules, atomic clusters, and ultracold atomic gases. In particular, some of these quantum systems exhibit quenching of the moments of inertia from their rigid-body values at very low temperatures. For over half a century, superfluidity has been studied in both fermionic, e.g., atomic nuclei [1], and bosonic, e.g., liquid ^{4}He [2], systems. For fermionic systems, pairing is central to superfluidity. More recently, the nature of collective excitations and superfluidity of strongly interacting Fermi gases has been of active interest [3–9]; nearly perfect irrotational flow with a quadratic dependence on the deformation has been observed by Clancy et al. [6]. With these recent advances, the moments of inertia of atomic nuclei warrant an updated investigation.

The standard approach to evaluating the empirical moments of inertia of atomic nuclei has been to assume an axially symmetric rotor with rotational energies given by $E(I) = AI(I+1)$, where $A = \hbar^2/(2\mathcal{J})$ and $\mathcal{J}$ is the moment of inertia. For $I^\pi = 2^+$, the energy reduces to $E(2^+) = 6A$ and $\mathcal{J} = 3\hbar^2/E(2^+)$. A further assumption is that the first $I^\pi = 2^+$ state is unmixed with other states. This approach is sufficient to demonstrate that moments of inertia of atomic nuclei fall between the rigid-body and irrotational flow values, as shown by Bohr and Mottelson in 1955 [1]. However, this approach is limited in validating microscopic calculations of moments of inertia and in elucidating the existence of any underlying symmetries. A more thorough understanding of inertial flow requires knowledge of all three components of the inertia tensor; this requires input beyond the energy of the first excited 2^+ state.

The description of low-lying excited states of deformed even–even nuclei has been largely based on collective rotations and vibrations about the average β and γ quadrupole shape parameters (cf. Ref. [10] for a thorough overview). These nuclei possess rotational bands built on the 0^+ ground states and relatively low-lying excited 2^+ states, which could be the result of triaxial rotations or γ vibrations; distinguishing the two is notoriously difficult but the latter interpretation has been traditionally adopted. Fortunately, the Kumar–Cline sum rules [11] provide an experimental means for determining the average quadrupole deformation values and variances. These sum rules have demonstrated that the average γ deformations, $<\gamma>$, are non-zero; an axially symmetric nucleus would give zero. Unfortunately, the variances of the quadrupole deformations are not typically known; these are needed to differentiate between rigid and soft deformation. The few cases where

* Corresponding author.
E-mail address: allmondjm@ornl.gov (J.M. Allmond).

http://dx.doi.org/10.1016/j.physletb.2017.01.072

the variances are known, e.g., the Os isotopes [12], lack precision but suggest that nuclei are neither rigid nor soft but somewhere in between.

We explore the implications of assuming β- and γ-rigid deformation (i.e., an axially asymmetric top) on the extracted moments of inertia. This is accomplished by using a recently formulated version of the triaxial rotor model with independent electric quadrupole and inertia tensors [13]; this is the simplest possible non-trivial view that allows a unique analytical solution to the three moments of inertia within the spin-2 subspace. While there have been investigations into the moments of inertia of axially asymmetric nuclei before, e.g., Refs. [14–18], empirical values for all three axes, to our knowledge, have never been reported.

In this Letter, empirical moments of inertia, $\mathcal{J}_1, \mathcal{J}_2, \mathcal{J}_3$, of 12 atomic nuclei with $E(4_1^+)/E(2_1^+) > 2.7$ are extracted from experimental $2^+_{g,\gamma}$ energies and electric quadrupole matrix elements, and the results are compared to expectations based on rigid and irrotational inertial flow. The $E2$ matrix elements used in this study are from multiple-step Coulomb excitation data [12,19–26], most of which are from the past two decades. Only by having the signs of the $E2$ matrix elements, i.e., $\langle 2^+_g||\hat{M}(E2)||2^+_g\rangle$ and $\langle 0^+_g||\hat{M}(E2)||2^+_g\rangle\langle 2^+_g||\hat{M}(E2)||2^+_\gamma\rangle\langle 2^+_\gamma||\hat{M}(E2)||0^+_g\rangle$, can a unique solution to all three components of the inertia tensor be obtained.

The Hamiltonian for rotations about three axes (i.e., an asymmetric top) is

$$H = A_1\hat{I}_1^2 + A_2\hat{I}_2^2 + A_3\hat{I}_3^2, \tag{1}$$

where the parameters A_1, A_2, A_3 are related to the components of the inertia tensor by $A_1 = \hbar^2/(2\mathcal{J}_1)$, $A_2 = \hbar^2/(2\mathcal{J}_2)$, $A_3 = \hbar^2/(2\mathcal{J}_3)$ and $\hat{I}_1, \hat{I}_2, \hat{I}_3$ are the angular momentum operators in the body-fixed frame with a $|IK\rangle$ basis. The Hamiltonian can be rewritten as

$$H = A\hat{I}^2 + F\hat{I}_3^2 + G(\hat{I}_+^2 + \hat{I}_-^2), \tag{2}$$

where

$$A = \frac{1}{2}(A_1 + A_2),\ F = A_3 - A,\ G = \frac{1}{4}(A_1 - A_2), \tag{3}$$

and

$$\hat{I}_\pm = \hat{I}_1 \pm i\hat{I}_2. \tag{4}$$

When applied to doubly-even nuclei, there is an $I^\pi = 0^+$ ground state with $E(0^+) = 0$, no $I^\pi = 1^+$ state, and two mixed $I^\pi = 2^+$ states ($K^\pi = 0^+, 2^+$) with energies given by

$$H(2^+) = \begin{pmatrix} 6A & 4\sqrt{3}G \\ 4\sqrt{3}G & 6A + 4F \end{pmatrix}, \tag{5}$$

which yields

$$E(2^+) = 6A + 2F \pm 2\sqrt{F^2 + 12G^2}. \tag{6}$$

The mixing angle is related to G and F by

$$\tan 2\Gamma = 2\sqrt{3}\frac{G}{F} \tag{7}$$

(note, $\Gamma < 0$ because $G < 0$) and the resulting $E2$ matrix elements for the $I^\pi = 0^+, 2^+$ subspace are

$$\langle 0^+_g||\hat{M}(E2)||2^+_g\rangle = \sqrt{\frac{5}{16\pi}}\,Q_0\cos(\gamma + \Gamma), \tag{8}$$

$$\langle 0^+_g||\hat{M}(E2)||2^+_\gamma\rangle = \sqrt{\frac{5}{16\pi}}\,Q_0\sin(\gamma + \Gamma), \tag{9}$$

$$\langle 2^+_g||\hat{M}(E2)||2^+_\gamma\rangle = \sqrt{\frac{25}{56\pi}}\,Q_0\sin(\gamma - 2\Gamma), \tag{10}$$

and

$$\begin{aligned}\langle 2^+_g||\hat{M}(E2)||2^+_g\rangle &= -\sqrt{\frac{25}{56\pi}}\,Q_0\cos(\gamma - 2\Gamma) \\ &= -\langle 2^+_\gamma||\hat{M}(E2)||2^+_\gamma\rangle.\end{aligned} \tag{11}$$

The $E2$ matrix elements are described by three parameters, $Q_\circ$ (axial deformation), γ (axial asymmetry), and Γ (mixing angle). Further details can be found in Refs. [13,25,27–29]. While the 2^+ mixing angle, Γ, can be inferred from the excitation energies of higher spins, such an approach is not particularly sensitive and, more importantly, it does not lead to a unique empirical value.

Once the $Q_\circ$, γ, and Γ deformation and mixing parameters are determined from the experimental $E2$ matrix elements, the A, F, and G parameters of the Hamiltonian can be extracted exactly using the experimental 2^+ energies, viz.

$$F = \frac{E(2^+_\gamma) - E(2^+_g)}{4\sqrt{1 + \tan^2(2\Gamma)}}, \tag{12}$$

$$A = \frac{E(2^+_g) + E(2^+_\gamma) - 4F}{12}, \tag{13}$$

$$G = \frac{F}{2\sqrt{3}}\tan 2\Gamma, \tag{14}$$

where the empirical moments of inertia are

$$\mathcal{J}_1 = \frac{1}{2}\frac{\hbar^2}{A + 2G}, \tag{15}$$

$$\mathcal{J}_2 = \frac{1}{2}\frac{\hbar^2}{A - 2G}, \tag{16}$$

$$\mathcal{J}_3 = \frac{1}{2}\frac{\hbar^2}{A + F}. \tag{17}$$

It is important to stress that the signs of the $E2$ matrix elements are required to obtain a unique solution to all three components of the inertia tensor. In particular, $\langle 2^+_g||\hat{M}(E2)||2^+_g\rangle$ determines whether the electric quadrupole moment is prolate or oblate, and $\langle 0^+_g||\hat{M}(E2)||2^+_g\rangle\langle 2^+_g||\hat{M}(E2)||2^+_\gamma\rangle\langle 2^+_\gamma||\hat{M}(E2)||0^+_g\rangle$ determines whether $\gamma > |\Gamma|$ or $\gamma < |\Gamma|$.

The present results can be connected directly to results obtained using rigid and irrotational flow moments of inertia by

$$\mathcal{J}_{rigid,\,k} = B_{rigid}\left[1 - \sqrt{\frac{5}{4\pi}}\beta\cos\left(\gamma - k\frac{2\pi}{3}\right)\right] \tag{18}$$

and

$$\mathcal{J}_{irrot.,\,k} = 4B_{irrot.}\beta^2\sin^2\left(\gamma - k\frac{2\pi}{3}\right), \tag{19}$$

where $k = 1, 2, 3$, $B_{rigid} = \frac{2}{5}MR^2 = 0.0138 \times A^{5/3}$ ($\hbar^2$/MeV), $B_{irrot.} = \frac{3}{8\pi}MR^2 = 0.00412 \times A^{5/3}$ ($\hbar^2$/MeV), $\beta = Q_\circ\sqrt{5\pi}/(3ZR^2)$, and $R = 1.2A^{1/3}$ (fm). It is important to highlight the fact that the irrotational-flow component of the moment of inertia in Eq. (19) resides in the mass parameter, $B_{irrot.}$. The $\beta^2\sin^2\left(\gamma - k\frac{2\pi}{3}\right)$ dependence is not explicitly limited to irrotational flow but results from the SO(5) invariance of the Bohr Hamiltonian (which happens to be fulfilled by irrotational flow), cf. page 121 of Ref. [10].

The mixing strength can be determined from the moments of inertia by

$$\Gamma = \frac{1}{2}\tan^{-1}\left(\sqrt{3}\frac{\mathcal{J}_2 - \mathcal{J}_1}{\frac{2\mathcal{J}_1\mathcal{J}_2}{\mathcal{J}_3} - \mathcal{J}_2 - \mathcal{J}_1}\right), \tag{20}$$

Table 1
Summary of the $2^+_{g,\gamma}$ energies, deformation parameters, and moments of inertia. See text for details.

Nuclei	$E(2^+_g)$ (keV)[a]	$E(2^+_\gamma)$ (keV)[a]	$Q_\circ$ (eb)	β	γ°	Γ°	$\mathcal{J}_1$ ($\hbar^2$/MeV)	$\mathcal{J}_2$ ($\hbar^2$/MeV)	$\mathcal{J}_3$ ($\hbar^2$/MeV)[b]
^{110}Ru	240.7	612.9	3.41(12)	0.283(11)	29.0(48)	−10.7(48)	22.0(81)	8.1(11)	3.88(18)
^{150}Nd	130.2	1062.1[c]	5.23(6)	0.283(3)	10.4(1)	−0.8(1)	27.5(6)	19.8(3)	1.964[d]
^{156}Gd	89.0	1154.1[c]	6.67(31)	0.330(15)	7.9(4)	−1.1(3)	55.0(84)	24.2(16)	1.779(1)
^{166}Er	80.6	785.9	7.75(3)	0.346(1)	9.2(2)	−0.4(1)	42.2(15)	33.3(9)	2.635[d]
^{168}Er	79.8	821.1	7.78(22)	0.345(10)	8.4(3)	−0.4(2)	42.6(26)	33.6(16)	2.517[d]
^{172}Yb	78.7	1465.9[c]	7.80(38)	0.331(16)	4.9(7)	0.0(4)	38.3(72)	37.9(70)	1.389[d]
^{182}W	100.1	1221.4	6.24(13)	0.241(5)	10.0(2)	−0.5(2)	35.9(25)	25.7(13)	1.684[d]
^{184}W	111.2	903.3	6.10(12)	0.234(5)	11.3(3)	−0.6(2)	30.6(15)	24.1(9)	2.309[d]
^{186}Os	137.2	767.5	5.58(8)	0.207(3)	20.4(7)	−2.4(7)	32.4(45)	16.3(11)	2.777(5)
^{188}Os	155.0	633.0	5.25(3)	0.193(1)	19.9(3)	−3.0(2)	26.5(6)	15.1(2)	3.451(2)
^{190}Os	186.7	558.0	5.05(6)	0.184(2)	22.1(5)	−5.9(5)	24.1(10)	11.7(2)	4.078(11)
^{192}Os	205.8	489.1	4.81(3)	0.174(1)	25.2(5)	−8.7(5)	21.6(7)	10.5(2)	4.857(19)

[a] Precision to better than ±0.1 keV [31].
[b] The precision is necessary to reconstruct F and $E(2^+_\gamma)$; but is beyond any model significance.
[c] $2^+_\gamma = 2^+_3$.
[d] Precision better than given number of significant figures.

where $\Gamma \leq 0^\circ$ for $\mathcal{J}_1 \geq \mathcal{J}_2 \geq \mathcal{J}_3$. For irrotational flow, the mixing reduces to

$$\Gamma_{irrot.} = -\frac{1}{2}\cos^{-1}\left(\frac{\cos 4\gamma + 2\cos 2\gamma}{\sqrt{9 - 8\sin^2 3\gamma}}\right), \tag{21}$$

which leads to the standard Davydov–Filippov rotor model [30]. Note that the mixing strength for "irrotational flow" does not explicitly depend on the irrotational-flow mass parameter $B_{irrot.}$ of Eq. (19).

A summary of the $2^+_{g,\gamma}$ energies, deformation parameters, and moments of inertia for the 12 nuclei with $E(4^+_1)/E(2^+_1) > 2.7$, clear γ-band candidates, and the necessary multi-step Coulex data is given in Table 1. The experimental energies and $E2$ matrix elements used in this study are from ENSDF [31] and multiple-step Coulomb excitation data [12,19–26], respectively. These data span $A = 110$ to 192 and $\gamma = 4.9^\circ$ to 29.0°, consistent with the model-independent results of the Kumar–Cline sum rules [11]. It is interesting to highlight the absence of any oblate nuclei in Table 1. While prolate dominance was once considered a mystery, it is now understood that the particle–hole symmetry, and hence prolate–oblate symmetry, of nuclei hold only for nuclei with a single partially occupied spherical harmonic oscillator shell; in multi-shell spaces there is no such symmetry [32,33].

All γ-band collectivity is described here as axially asymmetric rotations because of the restricted degrees of freedom of the model; this allows a simple and unique analytical solution to the three moments of inertia within the spin-2 subspace. Within the model, only ^{172}Yb is near symmetric with $\gamma = 4.9(7)^\circ$, $\mathcal{J}_1 = 38.3(72)$ ($\hbar^2$/MeV), and $\mathcal{J}_2 = 37.9(70)$ ($\hbar^2$/MeV). It must be recognized that both triaxial and vibrational degrees of freedom may be involved and small values of Γ may be the model "image" of γ vibrations about axial symmetry. However, recent advances with the Algebraic Collective Model (ACM) [10,34] have demonstrated that rotational bands exhibit significant mixing effects when β- or γ-vibrational bands occur at low excitation energies, suggesting that the dominant character of the low-lying states may be triaxial with the vibrational excitations at higher energies. This viewpoint is consistent with the fact that the triaxial rotor model has been shown to reproduce much of the spectroscopic data (particularly quadrupole moments) for low to medium spin for ^{110}Ru, ^{166}Er, and $^{186-192}$Os [25–27].

It is important to stress caution on some of the extracted moments of inertia in Table 1. In particular, nuclei such as ^{150}Nd, ^{156}Gd, and ^{172}Yb possess low-lying $2^+_\beta = 2^+_2$ states that could mix with the $2^+_{g,\gamma}$ states. Further, generally speaking, shape coexistence [35] could potentially distort the extracted moments of inertia also through mixing.

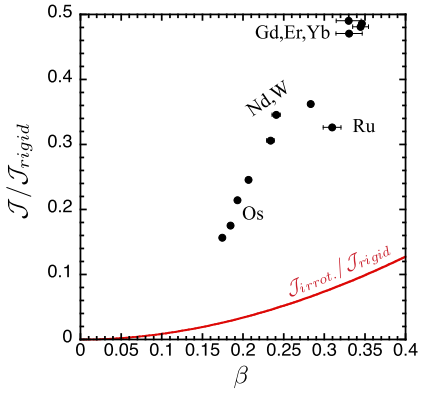

Fig. 1. The experimental (black) and irrotational (red) moments of inertia relative to the rigid-body value as a function of deformation, β, assuming $\mathcal{J} = \mathcal{J}_1 = \mathcal{J}_2$ and $\mathcal{J}_3 = 0$. (For interpretation of the references to color in this figure legend, the reader is referred to the web version of this article.)

Before analyzing the results of Table 1 in detail, it is important to note an historical point regarding the moments of inertia of atomic nuclei. As demonstrated before [1] and illustrated in Fig. 1, by assuming axial symmetry, the moments of inertia are found to be quenched to values between rigid and irrotational values. While this was a significant revelation, the one-dimensional perspective is limited in its ability to elucidate the nature of inertial flow; this will become evident upon the following 3-dimensional analysis.

The empirical moments of inertia for all three axes are shown in Fig. 2 relative to the leading-order rigid-body values, i.e., $\mathcal{J}_{rigid,k} \sim B_{rigid}$ from Eq. (18). The irrotational values are shown for comparison. The moments of inertia for all three axes remain quenched to values between the rigid and irrotational expectations. The three-dimensional view reveals that all three axes are qualitatively correlated with $\beta^2\sin^2(\gamma - 2\pi k/3)$, similar to irrotational flow (cf. discussion in the conclusion). The empirical moments of inertia for all three axes are shown in Fig. 3 relative to the irrotational-flow values. The experimental moments of inertia are on average a factor of 6.3, 7.4, and 10.0 larger than the irrotational flow values for the 1-, 2-, and 3-axis, respectively. The regularity in the three moments of inertia supports the triaxial assumption of the model. Despite the 3-axis having the smallest moment of inertia, there is no general indication that it is significantly more coupled to the intrinsic motion than the other

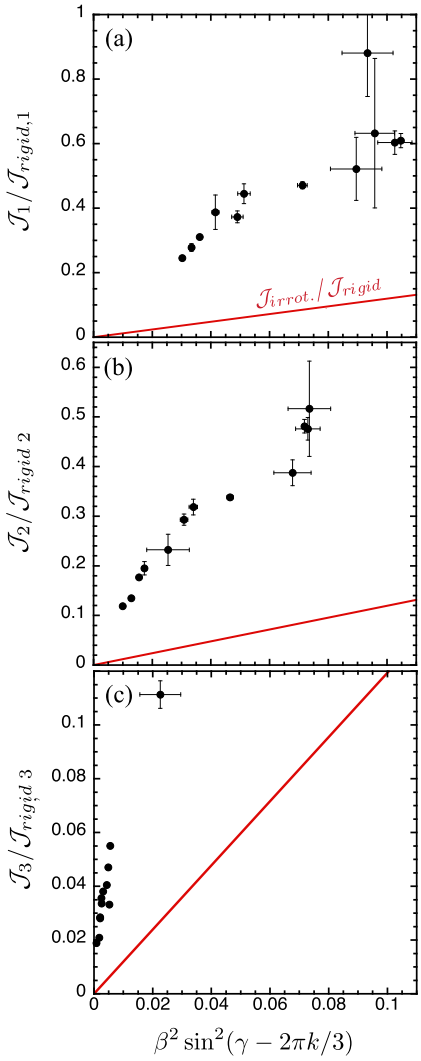

Fig. 2. The experimental (black) and irrotational (red) moments of inertia relative to the leading-order rigid-body value as a function of $\beta^2\sin^2(\gamma-2\pi k/3)$ for the 1-axis (a), 2-axis (b), and 3-axis (c), respectively. (For interpretation of the references to color in this figure legend, the reader is referred to the web version of this article.)

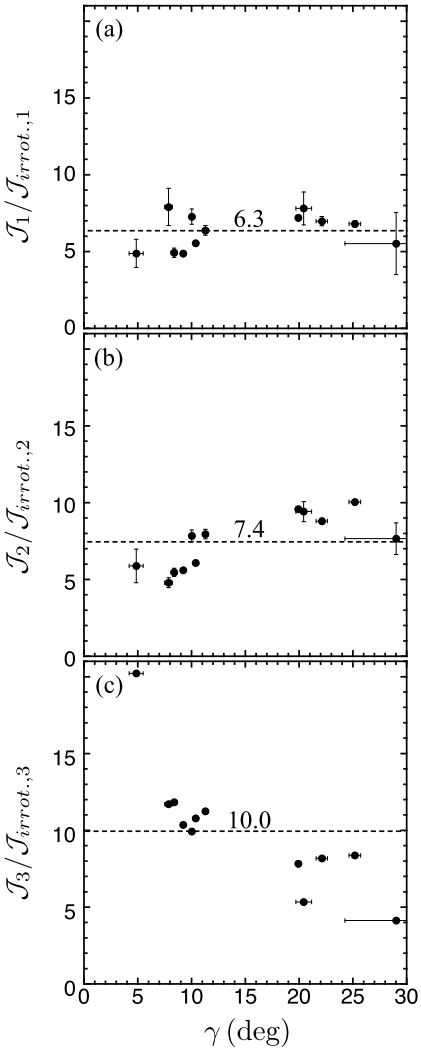

Fig. 3. The experimental moments of inertia relative to the irrotational flow value as a function of γ for the 1-axis (a), 2-axis (b), and 3-axis (c), respectively.

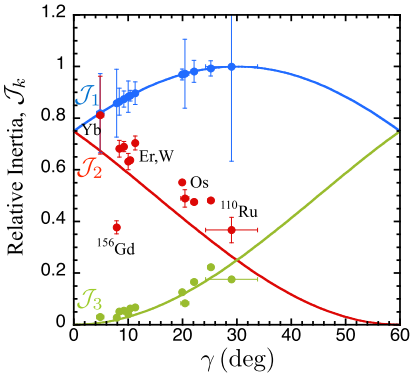

Fig. 4. The relative moments of inertia for all three axes as a function of axial asymmetry, γ. The experimental values (circles) have been normalized to the irrotational values (lines) through the 1-axis.

axes. However, the degree to which the 3-axis does deviate from the others, cf. the ^{172}Yb outlier at $\gamma = 4.9°$ in Fig. 3(c), may indicate a partial coupling to the intrinsic motion, expected for a γ vibration. Alternatively, the ^{172}Yb outlier may be the result of configuration mixing due to a relatively low-lying 0_2^+ band head; note that $2_\gamma^+ = 2_3^+$.

The relative moments of inertia as a function of axial asymmetry, γ, are shown in Fig. 4 for all three axes. The relative irrotational values are shown for comparison. Note the normalization of the scale to $\mathcal{J}_1$. The relative moments of inertia are qualitatively consistent with irrotational flow (cf. clarification in the conclusion). It is also clear $\mathcal{J}_1 > \mathcal{J}_2 \sim \mathcal{J}_3$ is manifested in nuclei that approach the triaxial limit of the electric quadrupole tensor, $\gamma = 30°$; this is a feature of the Bohr Hamiltonian that was pointed out by Meyer-ter-Vehn [36] in 1975 and it is now shown for the first time to be exhibited qualitatively by nuclei. Recent Coulomb excitation results of ^{110}Ru [26] establish it as the best candidate for triaxiality near the ground state to date. Additional Coulomb-excitation results for the neutron-rich Mo–Ru region with higher precision would be valuable. The outliers, ^{172}Yb and ^{156}Gd, correspond to cases with low-lying excited 0^+ states (with $K^\pi = 0^+, 2^+$ bands).

The empirical 2^+ mixing parameter, Γ, as a function of axial asymmetry, γ, is shown in Fig. 5(a). The rigid and irrotational values are shown for comparison. The experimental mixing strength reveals qualitative agreement with the irrotational flow expectation; this is due to the fact that the mixing is only dependent on the relative moments of inertia, which eliminates the explicit ir-

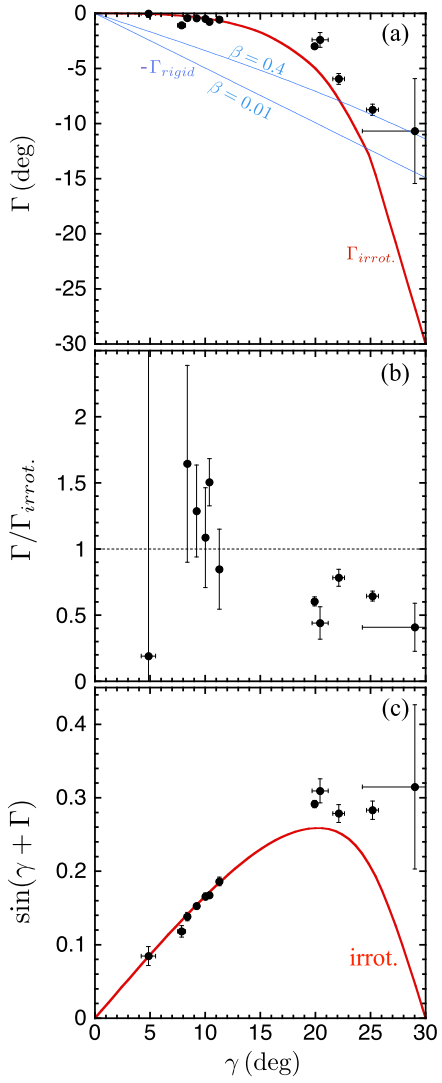

Fig. 5. (a) The experimental (black), irrotational (red), and rigid (blue) 2^+ mixing parameter, Γ, as a function of axial asymmetry, γ. (b) The ratio of the experimental and irrotational 2^+ mixing values. (c) The experimental (black) versus irrotational (red) $\sin(\gamma+\Gamma)$ values, which are proportional to $\langle 0_g||\hat{M}(E2)||2_\gamma\rangle$. (For interpretation of the references to color in this figure legend, the reader is referred to the web version of this article.)

rotational dependence $B_{irrot.}$ in Eq. (19). This explains the limited success (cf. Ref. [13]) of the Davydov–Filippov rotor model [30]. It is important to stress that, while there are some qualitative agreements in the relative moments of inertia with a $\beta^2\sin^2(\gamma-2\pi k/3)$ dependence, the quantitative moments of inertia on a case-by-case basis show significant deviations. Fig. 5(b) reveals the extent of the scatter of the 2^+ mixing values with respect to the "irrotational" values. These deviations can have a large impact on the calculated $E2$ matrix elements when approaching $\gamma=30°$ due to destructive interference [29], cf. Fig. 5(c), which reveals the discrepancy between the fitted and irrotational $\langle 0_g||\hat{M}(E2)||2_\gamma\rangle \propto \sin(\gamma+\Gamma)$ values. A $\beta^2\sin^2(\gamma-2\pi k/3)$ dependence of the moments of inertia is not sufficient in quantitative calculations [13].

We recognize that actual nuclei are believed to possess fluctuations in the β and γ shape parameters about average values. In some of the nuclei reported (chosen based on the availability of Coulex data, a clear γ-band candidate, and $E(4_1^+)/E(2_1^+)>2.7$), the present approach will be limited. This is particularly true for ^{150}Nd, ^{156}Gd, and ^{172}Yb which have low-lying 0_2^+ states. However, the variance in the shape parameters, which could equally result from configuration mixing, remains largely unknown experimentally and the present approach takes the simplest possible non-trivial view in extracting moments of inertia. We believe this will provide guidance to exploring, especially, γ-soft nuclei using a model such as the ACM [34], which will involve more parameters with concomitant difficulty in finding global minima in the fitting. However, it's important to recognize that within the ACM, low-lying β- and γ-vibrational bands result in unrealistically large mixing effects [10,34]; this fact in combination with the regularity of the 3 moments of inertia leaves one to conclude that the low-lying states are a composite of both triaxial and vibrational degrees of freedom with the former being the most likely dominant component. More precise Coulomb-excitation data, e.g., variances of quadrupole shape invariants, are needed to test this hypothesis.

A better description of inertial flow will require improving both the absolute and relative values. The absolute values are determined by the mass parameter B, cf. Eqs. (18) and (19); B_{rigid} is too large and B_{irrot} is too small. It is interesting to note that the relative moment of inertia values are qualitatively described by $\beta^2\sin^2(\gamma-2\pi k/3)$, cf. Fig. 2, which is a result of the SO(5) invariance [10,34] of the Bohr model [37,38]; irrotational flow is SO(5) invariant, but SO(5) invariance does not necessarily imply irrotational flow. Rowe et al. [34] have pointed out that a better description of inertial flow might be given within a collective model by the inclusion of vorticity degrees of freedom as done in superfluid hydrodynamics [39]. The symplectic model, $\mathrm{Sp}(3,\mathbb{R})$ [40], provides a promising step in this direction: it possesses vorticity degrees of freedom in one of its submodels and, moreover, it is a submodel of the shell model. It is also interesting to note that triaxial deformation naturally emerges within the symplectic model with low-lying collectivity being the result of mixing several triaxial rotor-like configurations [33].

While there have been significant advances in microscopic calculations [41–45], which include pairing interaction effects as suggested by Bohr, Mottelson, and Pines [46], the theoretical moments of inertia have been limited to one-dimensional comparisons without definitive evidence of axial symmetry. Furthermore, microscopic theories of deformed nuclei are often limited to ground-state calculations of the β and γ shape parameters, relying on a collective model to generate the excited states. A better understanding of inertial flow directly impacts the manner in which collectivity should be generated from predicted shape parameters. It is our hope that the new empirical moments of inertia for the 1-, 2-, and 3-axis of atomic nuclei further stimulate multiple-step Coulomb excitation experiments and algebraic and microscopic theory in the quest to better understand the nature of inertial flow in finite many-body quantum systems composed of strongly interacting fermions.

Acknowledgements

We gratefully acknowledge David Rowe and Thomas Papenbrock for fruitful discussions. This material is based upon work supported by the U.S. Department of Energy, Office of Science, Office of Nuclear Physics.

This manuscript has been authored by UT-Battelle, LLC under Contract No. DE-AC05-00OR22725 with the U.S. Department of Energy. The United States Government retains and the publisher, by accepting the article for publication, acknowledges that the United States Government retains a non-exclusive, paid-up, irrevocable, world-wide license to publish or reproduce the published form of this manuscript, or allow others to do so, for United States Government purposes. The Department of Energy will pro-

vide public access to these results of federally sponsored research in accordance with the DOE Public Access Plan (http://energy.gov/downloads/doe-public-access-plan).

References

[1] A. Bohr, B.R. Mottelson, Dan. Mat. Fys. Medd. 30 (1955) 1.
[2] G.B. Hess, W.M. Fairbank, Phys. Rev. Lett. 19 (1967) 216.
[3] K.M. O'Hara, S.L. Hemmer, M.E. Gehm, S.R. Granade, J.E. Thomas, Science 298 (2002) 2179.
[4] M. Bartenstein, A. Altmeyer, S. Riedl, S. Jochim, C. Chin, J.H. Denschlag, R. Grimm, Phys. Rev. Lett. 92 (2004) 203201.
[5] J. Kinast, A. Turlapov, J.E. Thomas, Phys. Rev. Lett. 94 (2005) 170404.
[6] B. Clancy, L. Luo, J.E. Thomas, Phys. Rev. Lett. 99 (2007) 140401.
[7] G.M. Bruun, H. Smith, Phys. Rev. A 75 (2007) 043612.
[8] S. Riedl, E.R.S. Guajardo, C. Kohstall, J.H. Denschlag, R. Grimm, New J. Phys. 13 (2011) 035003.
[9] H.J. Warringa, A. Sedrakian, Phys. Rev. A 84 (2011) 023609.
[10] D.J. Rowe, J.L. Wood, Fundamentals of Nuclear Models: Foundational Models, World Scientific Publishing Co., 2010.
[11] K. Kumar, Phys. Rev. Lett. 28 (1972) 249;
D. Cline, Annu. Rev. Nucl. Part. Sci. 36 (1986) 681.
[12] C.Y. Wu, et al., Nucl. Phys. A 607 (1996) 178.
[13] J.L. Wood, A.-M. Oros-Peusquens, R. Zaballa, J.M. Allmond, W.D. Kulp, Phys. Rev. C 70 (2004) 024308.
[14] N. Macdonald, Nucl. Phys. 14 (1960) 70.
[15] A.S. Davydov, N.S. Rabotnov, A.A. Chaban, Nucl. Phys. 17 (1960) 169.
[16] C.A. Mallmann, Nucl. Phys. 24 (1961) 535.
[17] P. Banerjee, S. Sengupta, Nucl. Phys. 61 (1965) 225.
[18] P. Banerjee, S. Sengupta, Nucl. Phys. 71 (1965) 634.
[19] B. Varnestig, thesis, Uppsala University, 1987.
[20] B. Kotliński, et al., Nucl. Phys. A 517 (1990) 365.
[21] C.Y. Wu, et al., Nucl. Phys. A 533 (1991) 359.
[22] C. Fahlander, et al., Nucl. Phys. A 537 (1992) 183.
[23] C. Fahlander, et al., Nucl. Phys. A 541 (1992) 157.
[24] N. Clarkson, thesis, University of Liverpool, 1992.
[25] W.D. Kulp, et al., Phys. Rev. C 73 (2006) 014308.
[26] D. Doherty, et al., Phys. Lett. B 766 (2017) 334.
[27] J.M. Allmond, R. Zaballa, A.M. Oros-Peusquens, W.D. Kulp, J.L. Wood, Phys. Rev. C 78 (2008) 014302.
[28] J.M. Allmond, J.L. Wood, W.D. Kulp, Phys. Rev. C 80 (2009) 021303(R).
[29] J.M. Allmond, J.L. Wood, W.D. Kulp, Phys. Rev. C 81 (2010) 051305(R).
[30] A.S. Davydov, G.F. Filippov, Nucl. Phys. 8 (1958) 237.
[31] Evaluated Nuclear Structure Data File (ENSDF), http://www.nndc.bnl.gov/ensdf/.
[32] B. Castel, D.J. Rowe, L. Zamick, Phys. Lett. B 236 (1990) 121.
[33] D.J. Rowe, J. Phys. G: Nucl. Part. Phys. 43 (2016) 024011.
[34] D.J. Rowe, T.A. Welsh, M.A. Caprio, Phys. Rev. C 79 (2009) 054304.
[35] K. Heyde, J.L. Wood, Rev. Mod. Phys. 83 (2011) 1467.
[36] J. Meyer-ter-Vehn, Nucl. Phys. A 249 (1975) 111.
[37] A. Bohr, Dan. Mat. Fys. Medd. 26 (1952) 14.
[38] A. Bohr, B.R. Mottelson, Dan. Mat. Fys. Medd. 27 (1953) 16.
[39] S.J. Putterman, Superfluid Hydrodynamics, North-Holland, Amsterdam, 1974.
[40] G. Rosensteel, D.J. Rowe, Phys. Rev. Lett. 38 (1977) 10;
G. Rosensteel, D.J. Rowe, Ann. Phys. (NY) 104 (1980) 134.
[41] A.K. Kerman, N. Onishi, Nucl. Phys. A 361 (1981) 179.
[42] L. Próchniak, P. Quentin, D. Samsoen, J. Libert, Nucl. Phys. A 730 (2004) 59.
[43] J.A. Sheikh, G.H. Bhat, Y. Sun, G.B. Vakil, R. Palit, Phys. Rev. C 77 (2008) 034313.
[44] T. Nikšić, D. Vretenar, P. Ring, Prog. Part. Nucl. Phys. 66 (2011) 519.
[45] Y. Shi, C.L. Zhang, J. Dobaczewski, W. Nazarewicz, Phys. Rev. C 88 (2013) 034311.
[46] A. Bohr, B.R. Mottelson, D. Pines, Phys. Rev. 110 (1958) 936.